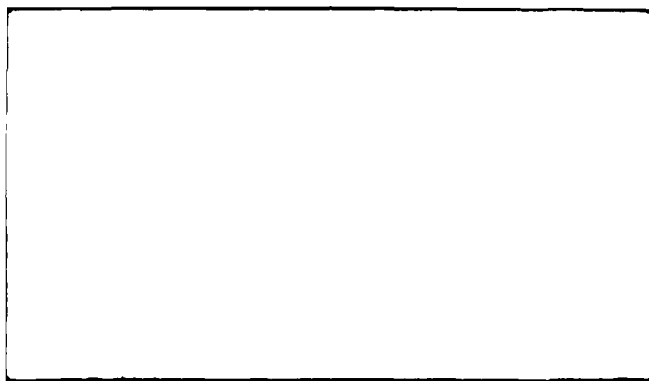END

DATE
FILMED

2-84

DTIC

MICROCOPY RESOLUTION TEST CHART

NATIONAL BUREAU OF STANDARDS 1963 A

R.P.I. Math. Report No. 139
November 7, 1983

Cochlear Mechanics:
Analysis for a Pure Tone

by

Mark H. Holmes and Julian D. Cole

Department of Mathematical Sciences

Rensselaer Polytechnic Institute

Troy, New York 12181

ABSTRACT

The dynamical response of a three-dimensional hydroelastic model of the cochlea is studied for a pure tone forcing. The basilar membrane is modeled as an inhomogenous, orthotropic elastic plate and the fluid is assumed to be Newtonian. The resulting mathematical problem is reduced using viscous boundary layer theory and slender body approximations. This leads to a nonlinear eigenvalue problem in the transverse cross-section. The solutions for the case of a rectangular and semi-circular cross-section are computed and comparison is made with experiment. The role of the place principle in determining the difference limen is presented and it is shown how the theory agrees with the experimental measurements.

INTRODUCTION

The theoretical and experimental basis for our understanding of the mechanical resolution of sound by the ear, principally as takes place in the cochlea, is currently undergoing an extensive reexamination. To understand why, it is necessary to outline how the basic system functions. After the signal is transmitted through the outer and middle ear it is received by the cochlea through the movement of the stapes, which is the last bone in the ossicular chain. This motion causes the fluid inside the cochlea to move which, in turn, stimulates waves to propagate down the basilar membrane (Fig. 1). This membrane widens, as well as decreases in thickness, so that the amplitude of the wave begins to grow and, at the same time, the wavelength decreases. However, because of damping, the wave eventually reaches a point on the membrane after which it quickly decays to zero. The location and absolute level of this maximum amplitude depends on the frequency; the higher the frequency the closer the location is to the stapes. The result of this dependence is a frequency map on the basilar membrane. It is thought that this leads to the mechanical resolution of the signal since there are sensory cilia setting on the membrane which respond to its deflection and transmit neural signals accordingly.

The problem with this form of mechanical resolution is that it does not seem to be sharp enough to explain the extremely fine tuning that is observed in the neural signals leaving the cochlea. This conclusion comes from experimental (Kiang et al,

1965; Geisler et al, 1974; Russell and Sellick, 1978) as well as theoretical (Zwislocki, 1965; Steele and Taber, 1979; Holmes, 1982) analysis of the system. It is for this reason that there has been a search in the last few years for a "second filter" to explain the fine tuning, but as of yet they have been unsuccessful (Frommer, 1979; Zwislocki, 1980; Lighthill, 1981; Khanna, 1983).

The problem is made more difficult by the current state of the experimental evidence that is available. Until recently some of the best results were obtained using Mossbauer measurements of the basilar membrane's motion (Johnstone and Boyle, 1967; Rhode, 1971). The procedure involves opening the cochlea, placing a radioactive source on the basilar membrane, and then measuring the response over several hours. Unfortunately, it appears that the radioactivity has a detrimental effect on the viability of the cells in a relatively short time (Kliauga and Khanna, 1983), and so, the results of these experiments are suspect. Moreover, the cochlea has an intricate defense mechanism and is, apparently, very sensitive to outside interference (Khanna and Leonard, 1981 and 1983). This means that the available experimental techniques used to date, including the laser interferometric measurements of Khanna and Leonard (1982), are probably only able to give a gross description of the normal response and are not capable of measuring the very fine tuning, if present, that is sought.

It is with this rather unsettling state of affairs that we consider the three-dimensional hydroelastic model for the

cochlea that is outlined below. Even though a considerable amount of work has been done on it (Steele, 1976; Chadwick and Cole, 1979; Steele and Taber, 1979; Holmes, 1980; Holmes, 1982) it has never been completely solved and probably never will except by tour de force numerical methods. It is therefore necessary to use certain approximations, such as boundary layer theory, to reduce the problem to a more tractable size. Steele (1974, 1976, 1980) has made significant contributions to the resolution of this problem and they have been the basis for much of our own work. His approach involves a WKB type of approximation of the solution, in which he specifies the shape of the transverse displacement of the basilar membrane. With this, energy methods and time averaged Lagrangians are used to find the eikonal and transport equations. Our approach, on the other hand, uses perturbation expansions of the original dif-ferential equations and systematic viscous boundary layer theory. Chadwick (1980) and Holmes (1982) have studied the fully three-dimensional problem in this way, but in doing so other assumptions such as high frequencies or a small mass density for the basilar membrane are imposed. We intend in this article to remove these restrictions and obtain the leading order approximation to the full hydroelastic problem for a pure tone forcing. As with any mathematical formulation of a complex physical problem, various assumptions are made concerning the structure and composition of the system, but they include most of these earlier models.

FORMULATION OF MODEL

We will assume the geometrical structure of the cochlea to be such that it consists of an unrolled tapered tube containing two fluid chambers. The partition separating these chambers consists of a rigid portion (the bony shelf), a flexible portion (the basilar membrane), and an aperture at the apical end (the helicotrema). The variability of the geometry is arbitrary except that we will assume the cochlear wall to be symmetric through the partition, in this case, through the x,y plane. The cochlear wall, along with the shelf, are rigid except at the basal end where there are two openings (the oval and round windows) that are covered by flexible membranes. The footplate of the stapes is attached to the cochlea at the oval window.

Although the assumptions made on the geometry are not unreasonable, they do impose limitations on the theory. The spiraling of the cochlea is neglected as it is believed to effect the response at only the lowest frequencies and is primarily for "packaging purposes " Also, the two chambers are not exactly symmetric and there is a third chamber, the scala media, which accounts for about 8% of the total volume. The possible effect of this third chamber has been studied by Adjemian (1981) and, although the results are incomplete, it does not appear to have a significant effect on the mechanical response of the system. It is, however, important for the neural response because of the different cations that these chambers contain.
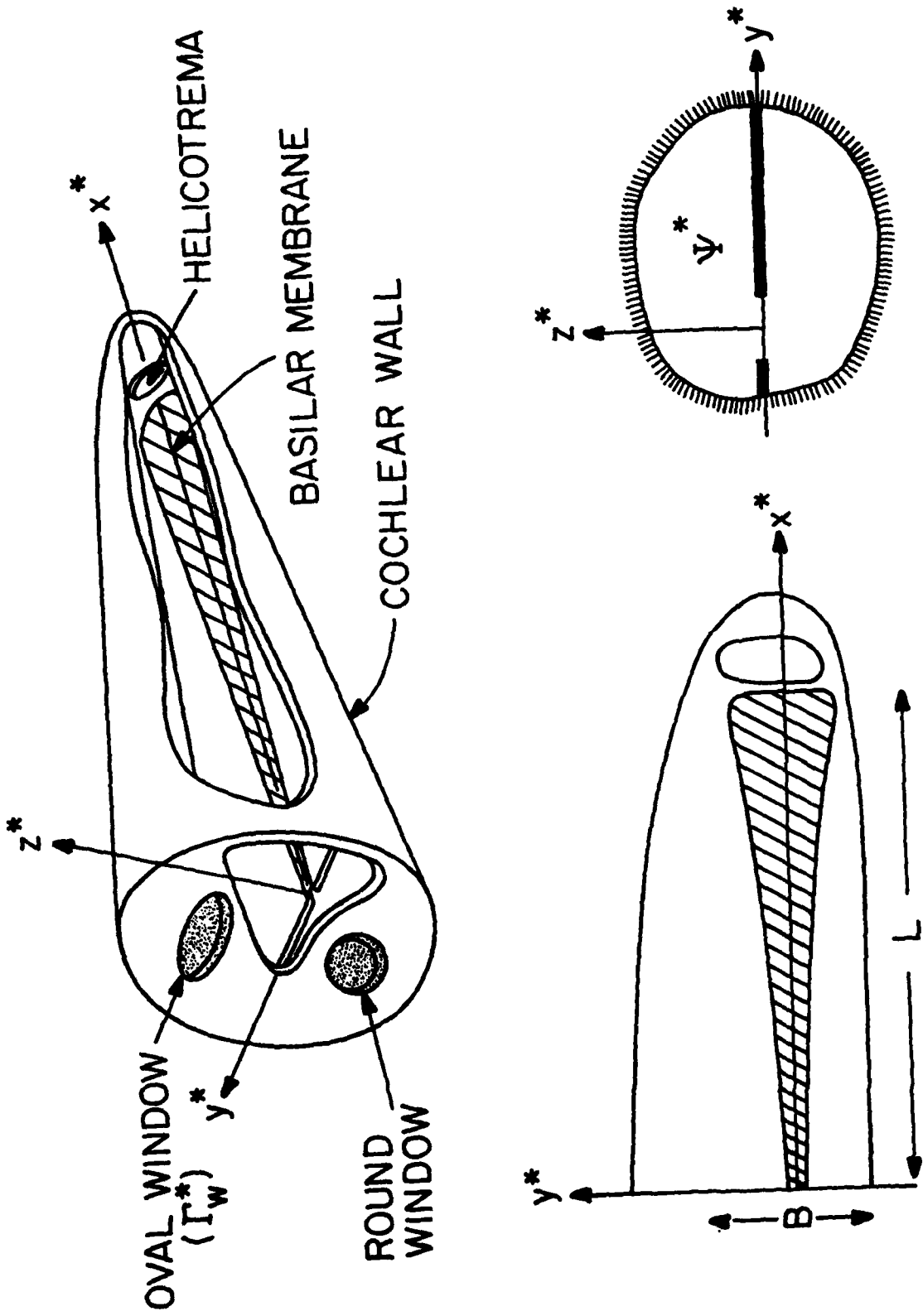
FIG. 1. The geometry and notation used for the hydroelastic model of the cochlea.

The fluid, called perilymph, that fills the two chambers is similar in terms of its mechanical response to water (Money et al, 1966; Rauch and Rauch, 1974). Consequently, it is considered to be Newtonian. Compressibility is omitted, even though the frequencies in the audible range can extend up to 15,000 Hz, as the overall length of the cochlea is only about 3.5 cm and the pressures at the stapes are relatively small (Lighthill, 1981). The fluid in the scala media, called endo-lymph, contains a relatively large concentration of proteins (Schuknecht, 1970; Rauch and Rauch, 1974). These macromolecules could very well have a significant effect on the response but are neglected in our study. Also, the convective terms in the Navier-Stokes equations are not included in our analysis. The reason is that, after scaling the problem, one finds that these nonlinear terms, relative to those obtained, are on the order of the ratio of the stapes amplitude to the cross-sectional width of the cochlea. For normal sound pressures this ratio is around 10^{-4} and so they do not contribute to the first term.

As for the basilar membrane, it is a composite material made up of an orthogonal weave of fibers and interspersed with ground substance (Iurato, 1967). From the studies of its elastic properties it appears to respond mechanically as an elastic plate (von Bekesy, 1960; Novoselova, 1975). Therefore, because of its fiber network and its variable thickness we will model it as an inhomogenous orthotropic elastic plate. It is not necessary to specify its exact location and configuration in the partition at this time as the analysis to follow applies to essentially any shape basilar membrane.

The remaining approximation concerns the relatively high frequencies in the auditory range (about 25 Hz or higher for the human cochlea). The Reynolds number, which is based on the width of the cross-section, is relatively large, and so, boundary layer theory can be used for the fluid. The error in this approximation is related to the curvature of the wall. In the examples to be considered later there are corners, but since they are isolated they do not interfere with the validity of the boundary layer approximation (Holmes, 1981).

The pressure of the fluid is represented by $p(x,y,z,t)$ and the vertical displacement of the basilar membrane is $\eta(x,y,t)$. In what follows both the independent and dependent variables are dimensionless, but, where necessary, an asterisk is used to indicate their dimensional analogue. So, for example, the nondimensional spatial coordinates x,y,z are related to x^*,y^*,z^* as follows

$$x^* = Lx \quad , \quad y^* = By \quad , \quad z^* = Bz \quad ,$$

where B and L are the characteristic width and length of the basilar memembrane respectively. As we are interested in the response to a pure tone let

$$p(x,y,z,t) = \bar{p}(x,y,z)e^{it} \quad ,$$

and

$$\eta(x,y,t) = \zeta(x,y)e^{it} \quad ,$$

where $t - .t^*$ and Ω is the given driving frequency. Also note tha'

$$p^*(x^*,y^*,z^*,t^*) = \rho A_s^* L\Omega^2 p(x,y,z,t)$$

and

$$n^*(x^*,y^*,t^*) = \left(\frac{\rho A_s^* L}{\mu_c}\right) n(x,y,t) \quad,$$

where A_s^* is the amplitude of the stapes, ρ is the fluid density, and μ_c is the mass per unit area of the basilar membrane at its center $(x=1/2)$. The pressure, because of the symmetry, is an odd function of z, and so, it is only necessary to consider the fluid motion in the upper chamber (Ψ).

From the above discussion we therefore have the following equations of motion:

i) for the fluid

$$(\epsilon^2\partial_x^2 + \partial_y^2 + \partial_z^2)\bar{p} = 0 \quad, \tag{1a}$$

ii) for the basilar membrane

$$\partial_y^2(D_2\partial_y^2\zeta) + \epsilon^2\left[\partial_y^2(\nu_1 D_2\partial_x^2\zeta) + \partial_x^2(\nu_1 D_2\partial_y^2\zeta) + 4\partial_x\partial_y(D_k\partial_x\partial_y\zeta)\right]$$

$$+ \epsilon^4\partial_x^2(D_1\partial_x^2\zeta) - \omega^2 h\zeta = -2\omega^2\bar{p}(x,y,0^+). \tag{1b}$$

The parameters are

$$\epsilon = \frac{B}{L} \qquad \text{and} \qquad \omega = \frac{\Omega}{\Omega_c} \quad,$$

where Ω_c represents a characteristic frequency of a beam in the cross-section and is given by

$$\Omega_c^2 = \frac{D_{2c}^*}{\mu_c B^4} \quad.$$

Here D_{2c}^* is the bending rigidity in the y-direction at the center of the basilar membrane. The functions D_1, D_2, and D_k are

the respective bending and twisting rigidities normalized by $D_{2c}*$, and ν_1 is the Poisson ratio characterizing the decrease in the y-direction during tension applied in the x-direction (Lekhnitskii, 1968). Also, $h(x,y)$ represents the thickness of the basilar membrane after normalization by h_c, which is the thickness at the center.

The kinematic boundary condition for the pressure (Appendix A), when $0<x<1$, is

$$(\partial_n - \beta\partial_n^2)\bar{p} = \begin{cases} -\alpha\zeta \text{ on the basilar membrane} \\ \\ 0 \text{ on the rigid wall ,} \end{cases} \tag{2}$$

where n represents the unit outward normal. The β term represents the viscous boundary layer correction to the inviscid boundary condition, where the constant β is given as

$$\beta^2 = \frac{\nu}{i\Omega B^2} ,$$

$$\alpha = \frac{\rho B}{\mu_c} ,$$

and ν is the kinematic viscosity of the fluid.

It is not necessary at the moment to specify the boundary conditions for the plate, but we will assume that it is either clamped or simply supported. Also, the boundary conditions at the basal and apical ends, where $x = 0,1$, are discussed later. It therefore remains to solve the above coupled system of partial differential equations to be able to describe the mechanical response to a pure tone.

TWO-VARIABLE EXPANSION

For most mammalian cochlae the aspect ratio ϵ is very small. For example, for humans it is on the order of 10^{-3}. We can take advantage of this through the use of a slender body approximation. For the case at hand, one finds that the appropriate expansions are

$$\bar{p} \sim \epsilon e^{-ik(x,\epsilon)} \left[\bar{p}_0(x,y,z) + \epsilon \bar{p}_1 + \ldots \right] \quad , \tag{3a}$$

and

$$\zeta \sim \epsilon e^{-ik(x,\epsilon)} \left[\zeta_0(x,y) + \epsilon \zeta_1 + \ldots \right] \quad , \tag{3b}$$

where

$$k(x,\epsilon) = \frac{\Theta(x)}{\epsilon} \quad .$$

Introducing these into (1), the $O(1)$ problem is found to be

$$(\partial_y^2 + \partial_z^2)\bar{p}_0 = \Theta_x^2 \bar{p}_0 \quad , \tag{4a}$$

and

$$\partial_y^2 (D_2 \partial_y^2 \zeta_0) - \Theta_x^2 \left[\partial_y^2 (\nu_1 D_2 \zeta_0) + \nu_1 D_2 \partial_y^2 \zeta_0 + 4 \partial_y (D_k \partial_y \zeta_0) \right]$$

$$+ (\Theta_x^4 D_1 - \omega^2 h)\zeta_0 = -2\omega^2 \bar{p}_0(x,y,0^+) \quad . \tag{4b}$$

As for the kinematic boundary condition (2), note that the boundary of the upper chamber can be parameterized as $y = \bar{y}(s,x)$, $z = \bar{z}(s,x)$ where $0<s<1$ represents the cross-sectional variation and $0<x<1$ the longitudinal. Thus the normal derivative in (2) expands as follows

$$\partial_n = \partial_{n_T} + \epsilon^2 b(x,s) \left[\partial_x - \frac{1}{2} b(x,s) \partial_{n_T} \right] + O(\epsilon^4) \quad ,$$

where n_T is the unit outward normal in the transverse cross-plane (x fixed) and

$$b(x,s) = - \vec{n}_T \cdot \left(\frac{\partial \bar{y}}{\partial x}, \frac{\partial \bar{z}}{\partial x}\right) \ .$$

With this and (2) we have that

$$(\partial_{n_T} - \beta \partial_{n_T}^2)\bar{p}_0 = \begin{cases} -\alpha\zeta_0 & \text{on BM} \\ 0 & \text{on rigid wall} \end{cases} \ . \tag{5}$$

To be definite we will now assume that the plate is simply supported, and so,

$$\zeta_0 = \partial_y^2 \zeta_0 = 0 \quad \text{for} \quad y = G_+(x), G_-(x) \ . \tag{6}$$

The boundary $y = G_+(x)$ represents the portion attached to the spiral lamina and $y = G_-(x)$ is the portion attached to the spiral ligament. It should be emphasized that clamped conditions, or a combination of simply supported and clamped boundary conditions could also be used.

The O(1) problem is now essentially complete. From it, it is only possible to determine uniquely θ_x^2 along with the y,z-dependence of ζ_0 and $\bar{p}_0$. It does not resolve the x-dependence of these variables and to do this one needs to consider the O(ϵ) problem. The details are outlined in Appendix B, and they basically involve integrating this higher order problem over the cross section. To simplify the expression we will consider the case of when the bending and twisting rigidities are independent of y, and are only functions of x. The result is that $\bar{p}_0$ and

ζ_0 have to be such that

$$\frac{d}{dx}\{\omega^2\Theta_x \iint_\psi \overline{p}_0^2 \, dydz + \alpha\Theta_x \int_{G_-}^{G_+} [D_1\Theta_x^2\zeta_0^2 + D_3(\zeta_{0_y})^2]dy\}$$

$$= -\beta\Theta_x \int_{\partial\psi} \partial_{n_T}(b\overline{p}_0^2) \quad , \tag{7}$$

where

$$D_3(x) = \nu_1 D_2 + 2D_k \quad .$$

To complete the problem we now need to consider the boundary conditions at $x = 0$ and at $x = 1$. At the basal end we have, using a boundary layer approximation as in (2), that

$$(\partial_x + \varepsilon\beta\partial_x^2)\overline{p} = \begin{cases} \overline{\eta} & \text{on oval window} \\ 0 & \text{on rigid portion,} \end{cases} \tag{8}$$

where $\overline{\eta}(y,z)$ represents the known displacement of the stapes footplate. To use this with the two-variable expansion (3) it is necessary to introduce an edge layer, with coordinate $\tilde{x} = x/\varepsilon$, and match the expansions in this region with (3). One finds that for the two expansions to match to the first order, mass must be conserved, and so, at $x = 0$ we require

$$\Theta_x(1 - i\beta\Theta_x) \iint_\psi \overline{p}_0 \, dydz = i\iint_{\Gamma_W} \overline{\eta} \, dydz \quad , \tag{9}$$

and

$$k(0,\varepsilon) = 0 \quad . \tag{10}$$

This omits the contribution of the basilar membrane which, because of its tapered geometry, is assumed to be negligible compared to the movement of the fluid in this region. Of special interest is the case of when $\overline{\eta} \equiv 1$, so that at $x = 0$

we require

$$\iint\limits_{\Psi} \bar{p}_0 \, dydz = \frac{iA_W}{\theta_x(1-i\beta\theta_x)} \quad , \tag{11}$$

where A_W represents the (normalized) area of the round window.

It would appear from (7) that there is only one constant of integration. However, there are at least two in the general solution since there are two values of $k(x,\epsilon)$ that are obtained from the square root of θ_x^2. In fact, the general solution consists of the superposition of the eigenfunctions obtained from (4). It is therefore necessary to introduce an edge layer at $x = 1$. However, by assuming the continuity of the pressure, and since it is an odd function of z, it follows that at the apical end

$$\bar{p}_0(1,y,z) = 0 \quad . \tag{12}$$

With this last boundary condition the problem for the first term approximation in (3) is essentially complete. It is centered around the unusual eigenvalue problem given in (4), θ_x^2 is the eigenvalue and $\bar{p}_0$, ζ_0 are the corresponding eigenfunctions. The problem is a nonlinear function of the eigenvalue θ_x^2 through the longitudnal bending and twisting rigidity terms in the equation for the basilar membrane as well as through the coupling with the fluid. It is also complex valued because of the viscous contribution in the kinematic boundary condition.

For use in the possible eigenfunction expansions to come from this problem, as well as for numerical approximations, it

is of interest to know the integral theorems. The simplest is
obtained by integrating (4) over the cross-section, from which
one finds that

$$\Theta_x{}^2(\iint_\Psi \overline{p}_0 \; dydz \; - \; \beta\int_{\partial\Psi} \overline{p}_0) \; = \; \alpha\int_{G_-}^{G_+} \zeta_0 \; dy \quad .$$

More important is the Rayleigh quotient, which is obtained by
multiplying by $\overline{p}_0$ and ζ_0 then integrating to obtain

$$\Theta_x{}^2(\iint_\Psi \overline{p}_0{}^2 \; dydz \; - \; \beta\int_{\partial\Psi} \overline{p}_0{}^2) \; = \; - \; \iint_\Psi [(\overline{p}_{0_y})^2+(\overline{p}_{0_z})^2]dydz \tag{13}$$

$$+ \; \frac{\alpha}{2\omega^2} \int_{G_-}^{G_+} [D_2(\zeta_{0_{yy}})^2 \; + \; 2D_3\Theta_x{}^2(\zeta_{0_y})^2 \; + \; \partial_y(\zeta_0{}^2)\partial_y(\nu_1 D_2)$$

$$+ \; (D_1\Theta_x{}^4 - \omega^2 h)\zeta_0{}^2]dy \quad .$$

This is, in effect, a relationship involving the kinematic and
potential energies of the system with the viscous dissipation.

SMALL β APPROXIMATION

Even though boundary layer theory was used to obtain (2) and (8), the fact that β is small was not considered in the two-variable expansions discussed in the last section. If we impose this on our eigenvalue problem there is a small, but important, simplification in the boundary conditions. To do this one finds that for small β

$$\theta_x \sim k_0(x) + \beta k_1(x) + \ldots \quad , \tag{14a}$$

$$\bar{p}_0 \sim p_0(x,y,z) + \beta p_1 + \ldots \quad , \tag{14b}$$

and

$$\zeta_0 \sim n_0(x,y) + \beta n_1 + \ldots \quad , \tag{14c}$$

Introducing these into (4) the following eigenvalue problem is obtained

$$(\partial_y{}^2 + \partial_z{}^2) p_0 = k_0{}^2 p_0 \quad , \tag{15a}$$

$$\partial_y{}^2(D_2 \partial_y{}^2 n_0) - k_0{}^2 [\partial_y{}^2(\nu_1 D_2 n_0) + \nu_1 D_2 \partial_y{}^2 n_0 + 4\partial_y(D_k \partial_y n_0)]$$

$$+ (k_0{}^4 D_1 - \omega^2 h) n_0 = -2\omega^2 p_0(x,y,0^+) \quad , \tag{15b}$$

where

$$\partial_{n_T} p_0 = \begin{cases} -\alpha n_0 & \text{on BM} \\ 0 & \text{on rigid wall} \end{cases} \tag{15c}$$

The viscous correction $k_1(x)$ in (14a) is found from the solvability condition for the $O(\beta)$ problem, which for the pressure is

$$(\partial_y{}^2 + \partial_z{}^2 - k_0{}^2) p_1 = 2k_0 k_1 p_0 \quad .$$

Multiplying this by p_0, integrating over the cross-section and then using Green's theorem one finds that

$$k_1(x) = \frac{k_0 \int_{\partial \Psi} p_0^2}{2 \iint_{\Psi} p_0^2 \, dy \, dz + \frac{2\alpha}{\omega^2} \int_{G_-}^{G_+} [D_3(\eta_{0_y})^2 + k_0^2 D_1 \eta_0^2] \, dy} . \tag{16}$$

As in (7), it has been assumed in deriving (16) that the bending and twisting rigidities are only functions of x. It is also of interest to note that this result can be obtained from the Rayleigh quotient by substituting (14) into (13). In any case, the complete first order approximation of the solution is then found by satisfying (7) along with the boundary conditions (6), (11), and (12).

SOLUTION OF NONLINEAR EIGENVALUE PROBLEM

Now that the original system of partial differential equations has been reduced using slender body and boundary layer theory it remains to solve the nonlinear eigenvalue problem (15). Once this is done it is a simple matter to find k_1 and satisfy the associated boundary conditions. To solve (15) one can use numerical methods, modal expansions , or Green's functions. Each has its advantages as well as its restrictions. We will illustrate the solution of the problem using the last two methods. The approach is similar for both methods since, for a given geometry, the eigenvalue problem is reduced to an integro-differential equation for $n_0(x,y)$ and $k_0(x)$. After this, Fourier expansions are used to reduce the problem to a set of algebraic equations that have k_0^2 as the eigenvalue and the Fourier coefficients as the eigenfunction. To facilitate the presentation we now assume that the plate is homogenous, so $D_2 = h = 1$, and D_1, D_3 are constants. However, both the width of the basilar membrane and the transverse cross section of the cochlea are still arbitrary functions of x.

Modal Expansions

For this case we assume that the cross-section is rectangular (Fig. 2). By separating variables in (15) one finds that

$$P_0(x,y,z) = \sum_{m=0}^{\infty} \bar{P}_m \cosh \lambda_m (H-z) \cdot \cos \gamma_m y \quad , \tag{17}$$

where

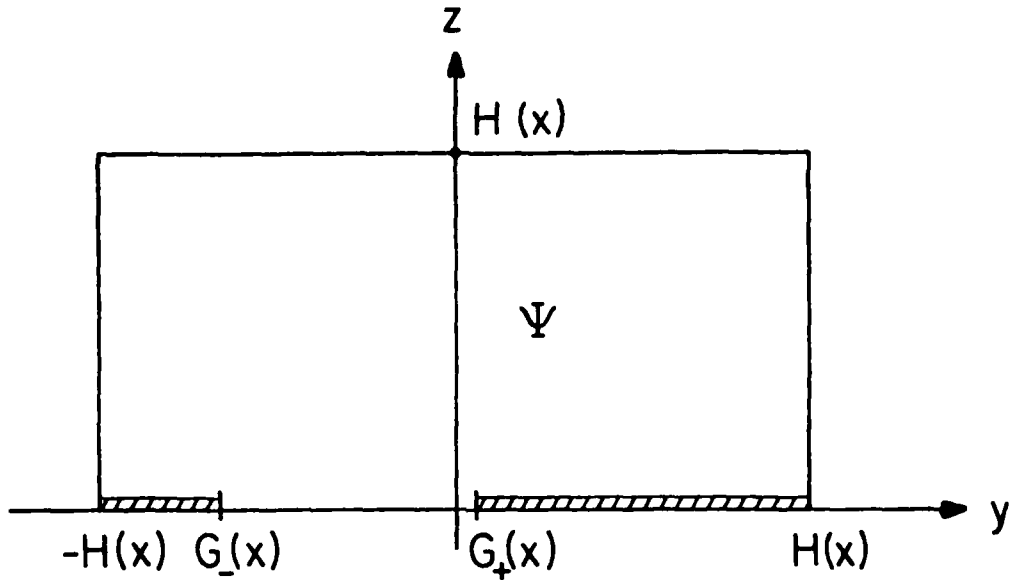$$\gamma_m = \frac{m\pi}{H} \quad , \qquad \lambda_m^2 = \gamma_m^2 + k_0^2 \quad ,$$

FIG. 2.   Transverse cross-section used for modal
expansion solution of eigenvalue problem.

and

$$\overline{P}_m = \frac{-\alpha c_m}{\lambda_m \sinh \lambda_m H} \int_{G_-}^{G_+} n_0 \cos \gamma_m s \, ds \quad ,$$

for

$$c_m = \begin{cases} \dfrac{1}{2H} & m = 0 \\[2ex] \dfrac{1}{H} & m \neq 0 \end{cases} \quad .$$

Substituting this into (15b) one obtains the following integro-

differential equation for k_0^2 and η_0

$$(\partial_y^4 - 2D_3 k_0^2 \partial_y^2 + D_1 k_0^4 - \omega^2)\eta_0 = \int_{G_-}^{G_+} L(x,y;s)\eta_0 ds \quad , \quad (18)$$

where

$$L(x,y;s) = \sum_{m=0}^{\infty} a_m(x)\cos\gamma_m y \cdot \cos\gamma_m s \quad ,$$

and

$$a_m = \frac{2\alpha\omega^2 c_m}{\lambda_m \tanh\lambda_m H} \quad .$$

To solve this we expand η_0 in modes as follows

$$\eta_0(x,y) = \sum_{n=1}^{\infty} b_n \cos\alpha_n [y - \left(\frac{G_+ + G_-}{2}\right)] \quad , \quad (19)$$

where

$$\alpha_n = \frac{\pi(2n-1)}{G_+ - G_-} \quad .$$

This satisfies the simply supported boundary conditions (6), and
for it to satisfy (18) one finds that the b_n's and k_0^2 have to
be such that

$$(\alpha_\ell^4 + 2D_3 k_0^2 \alpha_\ell^2 + D_1 k_0^4 - \omega^2)b_\ell = \frac{2}{G_+ - G_-} \sum_{m=0}^{\infty} \sum_{n=1}^{\infty} a_m b_n K_{mn} K_{m\ell} \quad ,$$

where

$$K_{mn} = \int_{G_-}^{G_+} \cos\gamma_m y \cdot \cos\alpha_n [y - \left(\frac{G_+ + G_-}{2}\right)] dy \quad .$$

We can write this set of equations in matrix form as

$$\overset{\rightarrow}{Mb} = \overset{\rightarrow}{0} \quad , \quad (20)$$

where $\underset{\sim}{M}$ is a nonlinear function of the eigenvalue k_0^2.

To find the solution it is necessary to know how many modes are needed for the pressure (17) and basilar membrane (19) to obtain a reasonable approximation. If the basilar membrane is in the center of the partition so that

$$G_+(x) = -G_-(x) = G(x) \quad , \tag{21}$$

then numerical studies show that the first mode for the basilar membrane and the first five modes for the pressure are sufficient. However, if the basilar membrane is not centered, or if the problem is asymmetric in y for any reason (e.g., because of asymmetric boundary conditions) then it is necessary to use several modes for the basilar membrane.

For the case of a centered basilar membrane, the characteristic equation obtained with a one mode approximation in (19) is

$$(\omega_r^2 + 2D_3\omega_r k_0^2 + D_1 k_0^4 - \omega^2)G = \sum_{m=0}^{\infty} a_m K_{m1}^2 \quad , \tag{22}$$

where

$$\omega_r = \left(\frac{\pi}{2G}\right)^2 \quad , \tag{23}$$

and

$$K_{m1} = \begin{cases} \dfrac{2\sqrt{\omega_r}\cos\gamma_m G}{\omega_r - \gamma_m^2} & \text{if } \gamma_m^2 \neq \omega_r \\[2ex] G & \text{if } \gamma_m^2 = \omega_r \end{cases} \quad .$$

This problem is similar to the one obtained by Steele and Taber (1979) using the method of averaged Lagrangians.

Green's Function

For this approach we will take a semi-circular cross-section and a centered basilar membrane (Fig. 3). The Green's function $G(x,y,z;y',z')$ satisfies

$$(\partial_{y'}^2 + \partial_{z'}^2 - k_0^2)G = \delta(y'-y)\delta(z'-z) \quad,$$

where

$$\partial_{n'_T}G = 0 \quad \text{along } \partial\Psi' \quad. \tag{24}$$

From this and (15a) it follows that

$$p_0(x,y,z) = 2\alpha\int_{-G}^{G} G(x,y,z;y',0)\eta_0(x,y')dy' \quad. \tag{25}$$

To find G recall that the fundamental solution of (15a) is the modified Bessel function K_0, and so,

$$G(x,y,z;y',z') = \frac{-1}{2\pi}K_0(|k_0|\sqrt{(y-y')^2+(z-z')^2}) + g(x,y,z;y',z') \quad,$$

where the function g satisfies (15a) and is such that G satisfies (24). Therefore,

$$g(x,y,z;y',z') = \frac{K_0'(k_0R)I_0(k_0r)I_0(k_0r')}{I_0'(k_0R)}$$

$$+ 2\sum_{n=1}^{\infty} \frac{K_n'(k_0R)I_n(k_0r)I_n(k_0r')}{I_n'(k_0R)}\cos(n\theta)$$

where $r = \sqrt{y^2+z^2}$, $r' = \sqrt{(y')^2+(z')^2}$, and θ is the angle between (y',z') and (y,z) with respect to the origin.
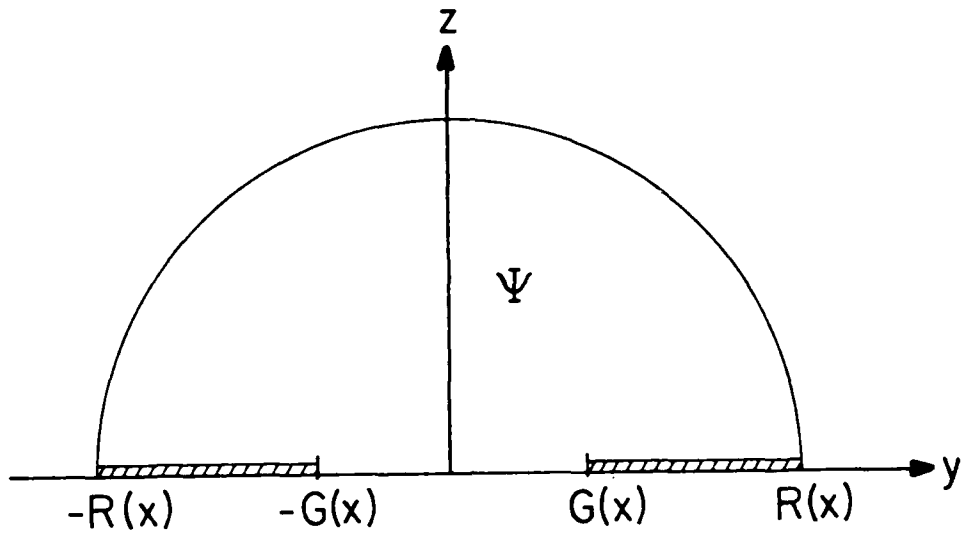
FIG. 3. Transverse cross-section used for Green's
function solution of eigenvalue problem.

With this it therefore follows that η_0 satisfies the integro-differential equation

$$(\partial_y^4 - 2D_3 k_0^2 \partial_y^2 + D_1 k_0^4 - \omega^2)\eta_0 = -2\alpha\omega^2 \int_{-G}^{G} K(x,y;s)\eta_0 ds \quad , \quad (26)$$

where

$$K(x,y;s) = -\frac{1}{2\pi} K_0(|k_0||y-s|) + g(x,y,0;s,0) \quad .$$

It is possible to simplify this by using the approximation

$k_0 R \gg 1$, which is the case of interest in the examples to be discussed later. Using the usual approximations for Bessel functions of large argument and the identity

$$I_0(w) = \sum_{-\infty}^{\infty} (-1)^n I_n(S) I_n(\sigma) e^{in\phi} \quad , \quad \text{where } w = (S^2 + \sigma^2 - 2S\sigma \cos \phi)^{1/2},$$

the eigenvalue problem becomes

$$(\partial_y^4 - 2D_3 k_0^2 \partial_y^2 + D_1 k_0^4 - \omega^2) \eta_0 = \frac{2\alpha\omega^2}{\pi} \int_{-G}^{G} f(y-s) \eta_0 ds \quad , \quad (27)$$

where

$$f(s) = K_0(|k_0 s|) + \pi e^{-2|k_0|R} I_0(|k_0 s|) \quad . \quad (28)$$

We have also assumed that the plate is centered (21).

For the first mode approximation of η_0, one finds that the characteristic equation for k_0^2 is

$$\omega_r^2 + 2D_3 \omega_r k_0^2 + D_1 k_0^4 - \omega^2 = \omega^2 G(x) F(\kappa_0, \kappa_1) \quad , \quad (29)$$

where

$$F(\kappa_0, \kappa_1) = \frac{8\alpha}{\pi} \int_0^1 \lfloor K_0(\kappa_0 s) + \pi e^{-\kappa_0 \kappa_1} I_0(\kappa_0 s) \rfloor \lfloor (1-s)\cos \pi s + \frac{1}{\pi}\sin \pi s \rfloor ds$$

$$(30)$$

for $\kappa_0(x) = 2|k_0| G(x)$ and $\kappa_1(x) = R(x)/G(x)$. It remains to solve this equation for k_0, but it is of interest to note that the effect of the outer boundary is contained entirely in the exponential term in (30) through the ratio of the half width of the basilar membrane to the cross-sectional radius.

NUMERICAL RESULTS

To illustrate the quantative nature of the solution let
B = 0.05 cm, L = 3.5 cm, ν = 0.008 cm/sec, and ρ = 1.0 gm/cm^3.
Also, $\mu = h_c \rho_c$ and

$$D_{2c}{}^* = \frac{E_2 h_c{}^3}{12(1-\sigma^2)} \quad ,$$

where E_2 = 4X10^6 dyn/cm^2, h_c = 3.8 X 10^{-3} cm, and σ = 1/2. The
boundary of the basilar membrane is given as

$$G(x) = \frac{1}{12}(5x+1) \quad , \qquad 0 < x < 1 \quad ,$$

and the cross-sectional area is assumed to have a constant value
of 0.01 cm^2, which determines H and R in Figs. 2 and 3. Although
we have not attempted to be absolutely realistic, these values
are representative of those found for the human cochlea (Holmes,
1980).

Before discussing the full solution we first consider the
effect of the bending and twisting rigidities of the plate, as
well as the shape of the cross-section, on the eigenvalue $k_0{}^2$.
In Fig. 4 the values obtained using (22) are shown for the case
of an isotropic plate, where D_1 = D_3 = 1, and a strongly ortho-
tropic plate, with D_1 = D_3 = 0, for a driving frequency of
1800 Hz. Also shown are the values obtained for a
semi-circular cross-section for the strongly orthotropic plate.
In this figure, as well as in all that follow, eight pressure
modes are used in (17) and (22). From this result one can see
that the effect of an orthotropic plate is not significant near
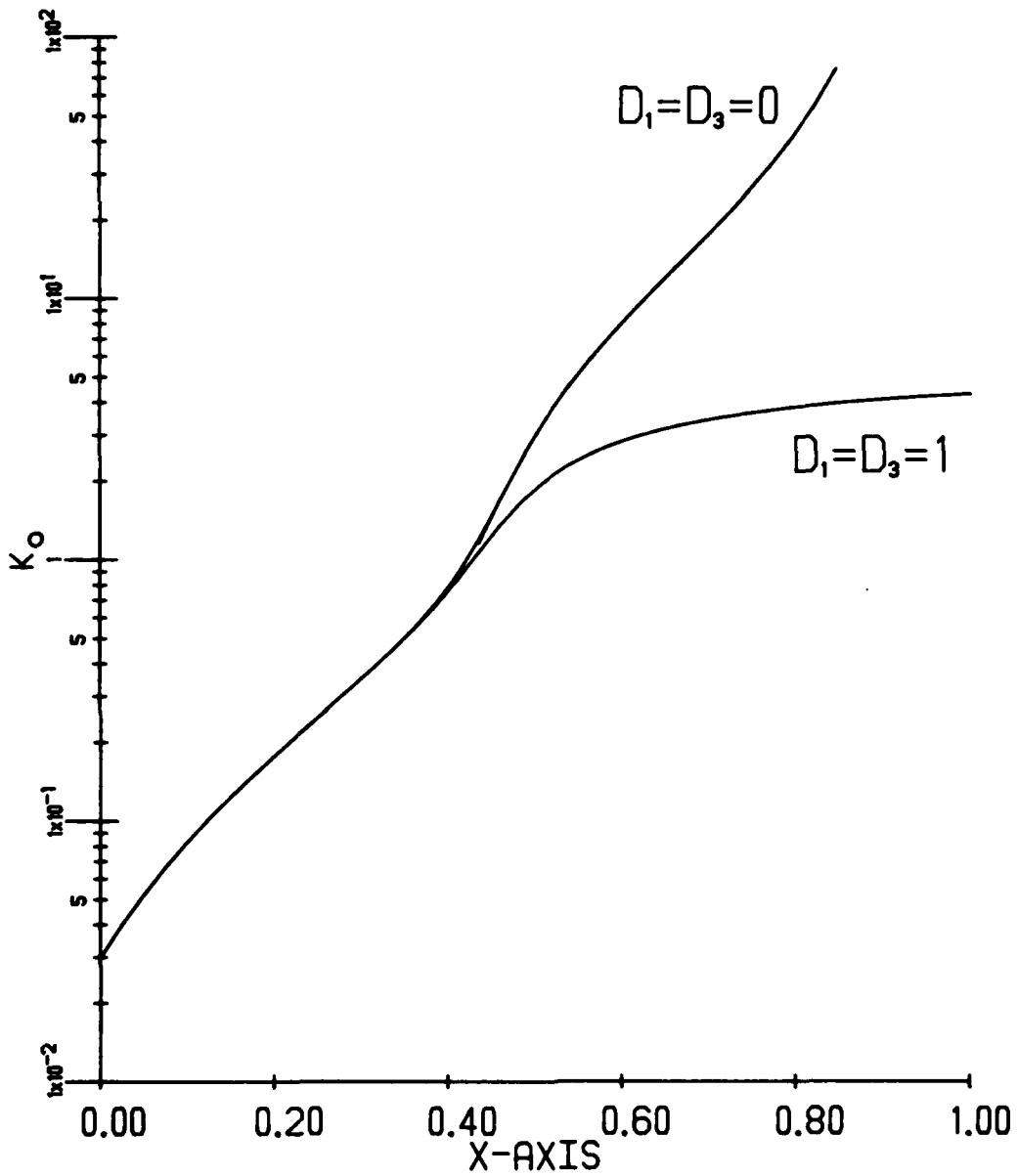
FIG. 4. The eigenvalue $k_0(x)$ as a function of longitudinal
position for a driving frequency of 1800 Hz. Shown
are the values for a rectangular cross-section (22)
with $D_1=D_3=1$, lower curve, and with $D_1=D_3=0$, upper
curve. Also, shown is the solution for a circular
cross-section (29) with $D_1=D_3=0$, which is essentially
indistinguishable from the analagous curve for a
rectangular cross-section.

the basal end, $x = 0$, as the wavenumber is still relatively small. However, as the wavelength decreases, so x increases, the longitudinal bending terms have a substantial effect on the eigenvalue. In other words, the smaller the wavelength the more important the longitudinal coupling is in the basilar membrane. This difference also changes the damping in the sense that the smaller the eigenvalue the less the viscous dissipation of the wave (16). As for a rectangular and circular cross-section, the curves in the figure are indistinguishable. Equation (29) was used to calculate the semi-circular geometry, but only for $k_0 > 1$, as was assumed in the derivation.

There have been a number of studies on the elastic properties of the basilar membrane which, unfortunately, usually involve relatively large amplitude deformations (von Bekesy, 1960; Voldrich, 1978). However, it appears that the longitudinal coupling is relatively weak, and so, in the next examples it is assumed that the basilar membrane is strongly orthotropic, which means that $D_1 = D_3 = 0$. In this case it is a simple matter to prove that k_0^2 is real since, from (13), one finds that

$$k_0^2 \iint_\Psi |p_0|^2 \, dydz = -\iint_\Psi |\nabla p_0|^2 \, dydz + \frac{\alpha}{2\omega^2} \int_{G_-}^{G_+} |\eta_{0_{yy}}|^2 \, dy \quad .$$

In the examples discussed here there is only one positive eigenvalue, which leads to left and right traveling waves in (3). When the viscous correction is included, i.e., k_1, these waves are damped. For the parameter values given above, when the frequency is above about 600 Hz, it is not

necessary to include the left running wave as the apical
boundary condition is effectively satisfied by the one
traveling to the right. In the examples presented below the
reflected wave, that is, the one moving towards the stapes,
is not included.

With the assumption that the reflected wave is negligible
the solution, as given by (3), is relatively easy to find. To
do so it is also assumed that the problem is symmetric about the
z-axis, so that it is sufficient to only use the first mode in
(19). In this case the displacement of the basilar membrane is

$$n*(x,y,t) - A_s*\cdot A(x)e^{i\left[t-\pi/2-k(x,\varepsilon)\right]}\cos(\pi y/2G) \quad , \tag{31}$$

where

$$k(x,\varepsilon) = \frac{1}{\varepsilon} \int_0^x \left[k_0(s)+\beta_0 k_1(s)\right]ds \quad ,$$

$$A(x) = \frac{A_0}{\sqrt{k_0(x) \iint_\psi p_0^2 dydz}} \cdot e^{-\frac{1}{\varepsilon} \beta_0 \int_0^x k_1(s)ds} \tag{32}$$

$$A_0 = \frac{\pi A_w k_0(0)}{4G(0)} \sqrt{k_0(0) \iint_\psi p_0(0,y,z)^2 dydz} \quad ,$$

$\beta_0 = \delta/\sqrt{2}$, $A_w = A_w*/B^2$ is the (dimensionless) area of the
oval window, and A_s* is the amplitude of the stapes. The func-
tion $k_0(x)$ is determined from (22) for a rectangular cross-
sectional geometry and from (29) for a semi-circular cross-
section. After this, $p_0(x,y,z)$ is found from either (17) or
(25) and $k_1(x)$ is determined from (16). It is of interest to
note that (31) is equivalent, in terms of its functional form, to

the solutions obtained by Steele (1980) and by Lighthill (1983). However, their procedure to calculate the coefficients is, apparently, different so it is unclear how their solutions compare with ours.

The phase ph(x) of the wave in (31) is given as

$$ph(x) = -\frac{\pi}{2} - \frac{1}{\epsilon} \int_0^x \lfloor k_0(s) + \beta_0 k_1(s) \rfloor ds \quad . \tag{33}$$

The phase velocity $v^*(x)$ is therefore

$$v^*(x) = \frac{B\Omega}{k_0(x) + \beta_0 k_1(x)} \quad . \tag{34}$$

The function A(x) in (32) is the amplitude of the wave on the basilar membrane. To see how it depends on x note, from Fig. 4, that k_0 increases significantly with x. For large k_0 one can approximate the eigenvalue problem (29) with

$$D_1 k_0^4 + 2D_3 \omega_r k_0^2 + \omega_r^2 - \omega^2 = \frac{2\alpha\omega^2}{k_0} \quad . \tag{35}$$

Also, for large k_0 in (16)

$$k_1 \sim k_0^2 \tag{36}$$

and, from (17),

$$\frac{1}{\sqrt{k_0 \int\int p_0^2 dy \ dz}} \sim \left(\frac{\sqrt{2H\omega_r}}{\alpha} \right) k_0 \quad . \tag{37}$$

If $D_1 = D_3 = 0$ then

$$k_0 \sim \frac{2\alpha\omega^2}{\omega_r^2-\omega^2} \quad , \tag{38}$$

whereas, if $D_1=D_3^2\neq0$ then

$$k_0 = \left(\frac{\alpha\omega}{D_3}\right)^{1/3} + O(\omega_r-\omega) \quad . \tag{39}$$

This means that for the strongly orthotropic case (38), k_0 becomes infinite as x increases, that is, as $\omega_r = \left(\frac{\pi}{2G}\right)^2$ approaches ω. This represents the position of the transverse beam, in the basilar membrane, with a fundamental frequency corresponding to the given driving frequency. For an ortho-tropic case as in (39), k_0 has no singularity and simply increases continuously with x. The singular nature of the strongly orthotropic case results in a nonuniform expansion in (14). However, from (32) and (36), the solution decays exponen-tially as it enters this region. In fact, the place principal arises from the balance in (32) between the increase in the coefficient, as given in (37), and the exponential decay coming from (36) and (38). As the wave propagates down the basilar membrane the phase velocity decreases, and goes to zero as it approaches the singular point. This is reminiscent of the behavior associated with critical layer absorption as discussed by Lighthill (1981). It is also of interest to note that the large wavenumbers, as determined from (35), are altogether independent of the shape of the cross section. At the same time, the resonant point (38) would not exist without the fluid or without the mass of the basilar membrane.

In Fig. 5 the amplitude and phase of the wave propagating down the center of the basilar membrane (y=0) is shown for three driving frequencies (Appendix C). One can see that the amplitude at 600 Hz is not negligible at x = 1, which shows that it is necessary to include the reflected wave for lower frequencies. Also, the amplitude for all three frequencies is not zero at x = 0, which is the result of not including the contribution of the edge layer. If this were done there would only be a minor change in the curves, except for the very high frequencies which have a maximum near to this region. In any case, the amplitude curves show the usual shift towards the basal end as the frequency increases. Also, the amplitude increases from 75 at 600 Hz to 220 at 6000 Hz. In other words, the maximum amplitude of the basilar membrane is from 115 to 225 times the amplitude of the stapes for frequencies between 1000 and 10,000 Hz, which is consistent with the measurements of Rhode (1971) and Khanna and Leonard (1981). It is also interesting to note that in situ the amplitude of the stapes decreases, for a given sound pressure, as the frequency increases, which would tend to counteract this growth.

Tuning and phase curves are shown in Fig. 6, which represent the amplitude of the wave at a fixed location as a function of frequency. The points x = 0.82, 0.45, 0.20 are chosen as they represent the positions of the maximum amplitudes in Fig. 5. Overall, the curves show a relatively sharp tuning. Whether or
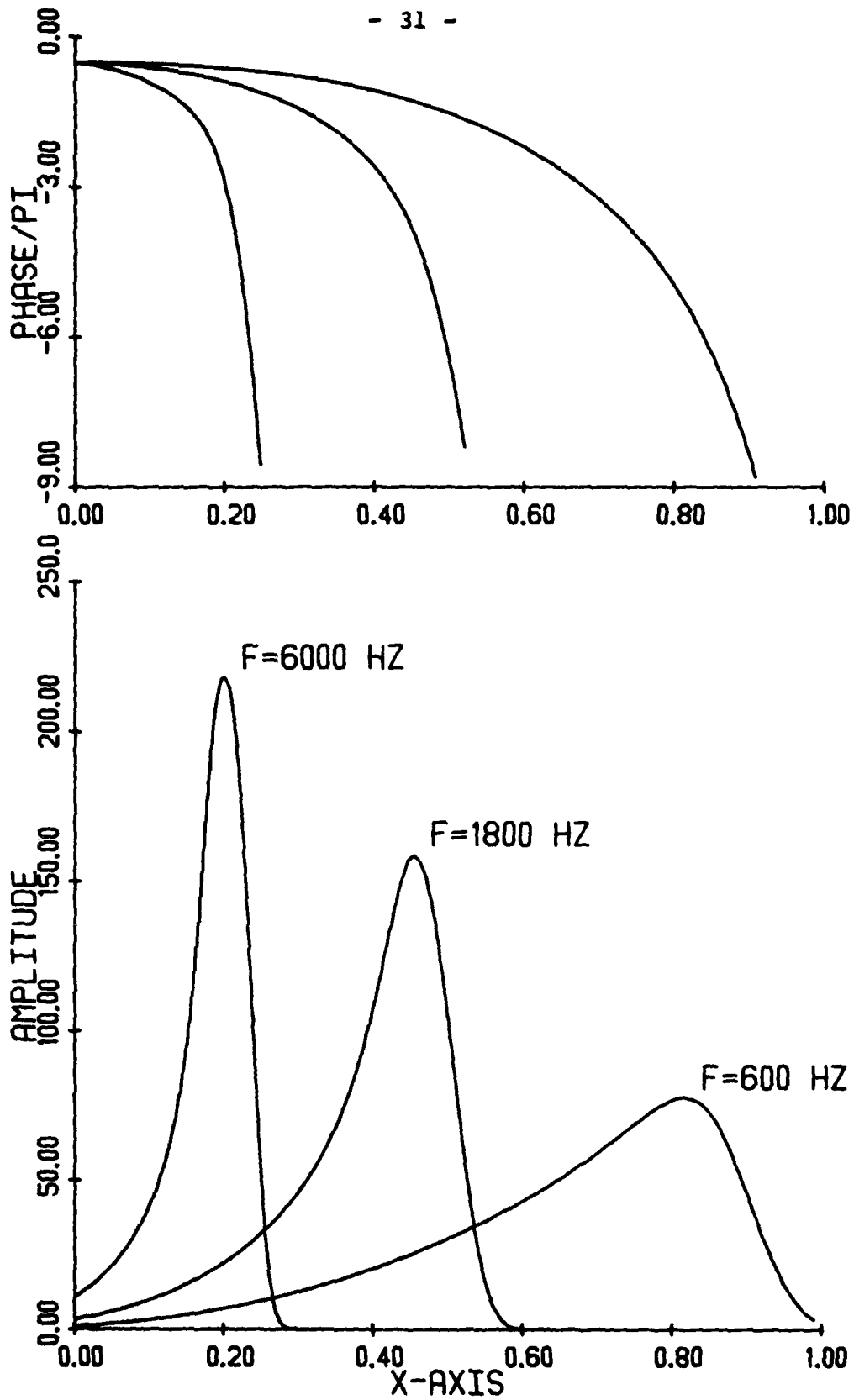
FIG. 5. The amplitude and phase of the wave on the basilar membrane, as a function of position, at three different driving frequencies.
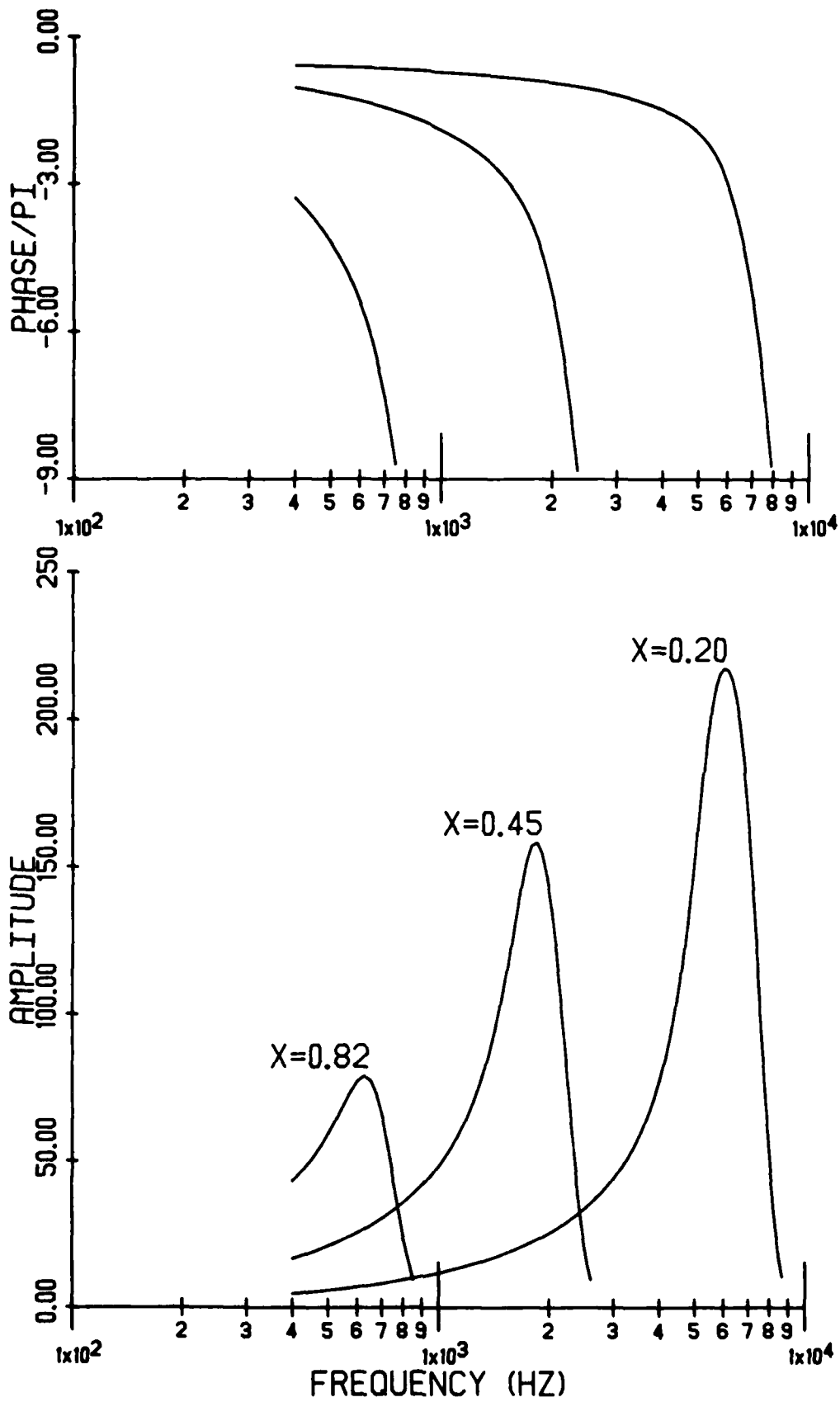
FIG. 6. The amplitude and phase of the wave on the basilar membrane, as a function of frequency. The three fixed spatial locations shown correspond to the points of maximum amplitude in Fig. 5.

not they are physiologically realistic is unclear but they are
significantly sharper than those obtained by von Bekesy (1960).
However, they are not as sharp as would be implied from the
neural tuning curves.

The phase velocities of the waves in Figs. 5 and 6 are
shown in Fig. 7, along with von Bekesy's (1960) measurements.
In Fig. 7a it is seen that the wave slows down as it propagates
down the basilar membrane, and significantly so once it begins
to approach the point of maximum amplitude. The values found
from the theory are smaller than those obtained by von Bekesy,
which he states (pg 458) "are representative of all the measure-
ments" made on cochlear models and cadevar specimens. From Fig.
7b, at a fixed spatial location, the phase velocity has a rela-
tive constant value until the frequency begins to approach the
frequency of largest amplitude for this point. When this occurs
the phase velocity decreases very rapidly as the frequency
increases.

It is rather easy to determine the position x_M of the max-
imum amplitude as a function of frequency. The result is shown
in Fig. 8, which also includes the measurements of Crowe, et al.
(1934) on the spatial localization based on pathological
condition, as well as von Bekesy's (1960) measurements on cada-
vers. It appears that in this aspect the theory agrees well
with experiment.

The last result concerns the difference limen (DL), or
just-noticeable-differences, obtained from the theory. These
represent the minimum change in the driving frequency for there

a)

VELOCITY (CM/SEC)

F=6000 HZ   F=1800 HZ   F=600 HZ

X-AXIS

b)

X=0.20

X=0.45

X=0.82

VELOCITY (CM/SEC)
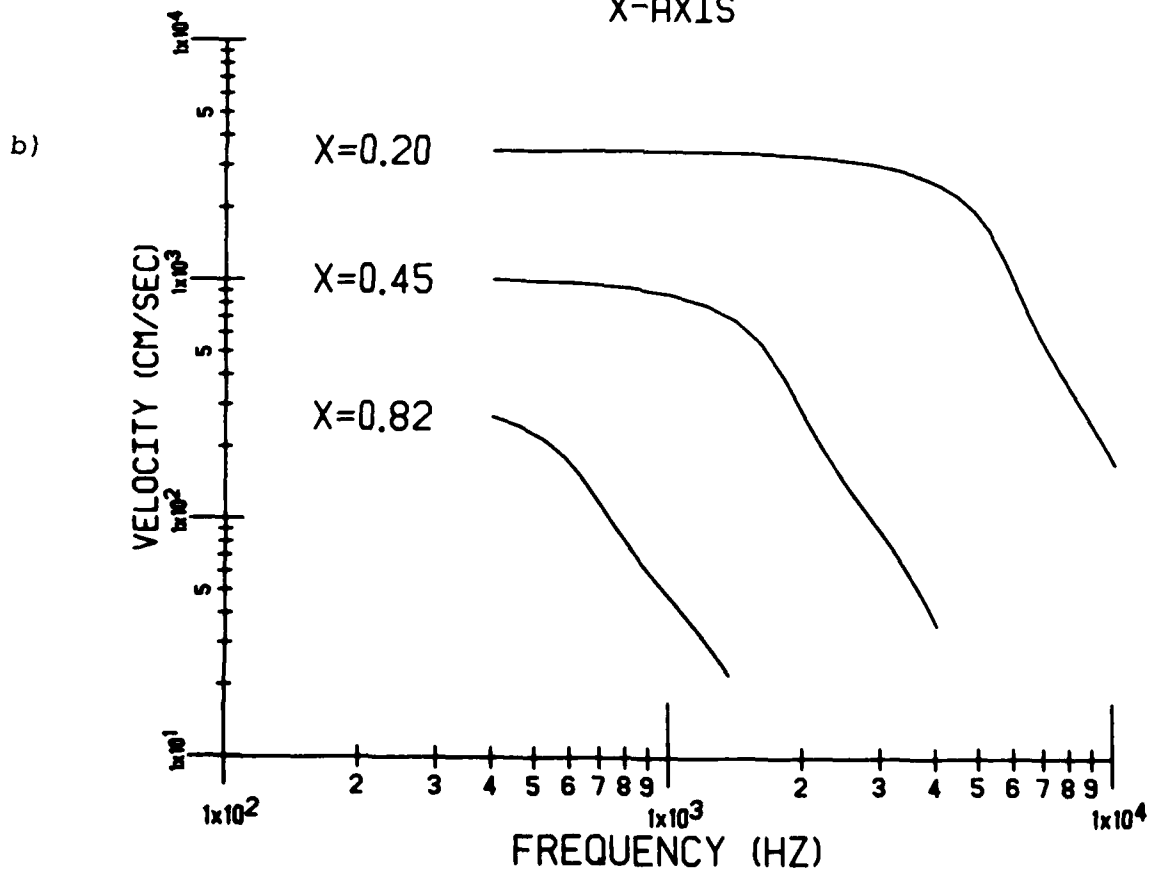
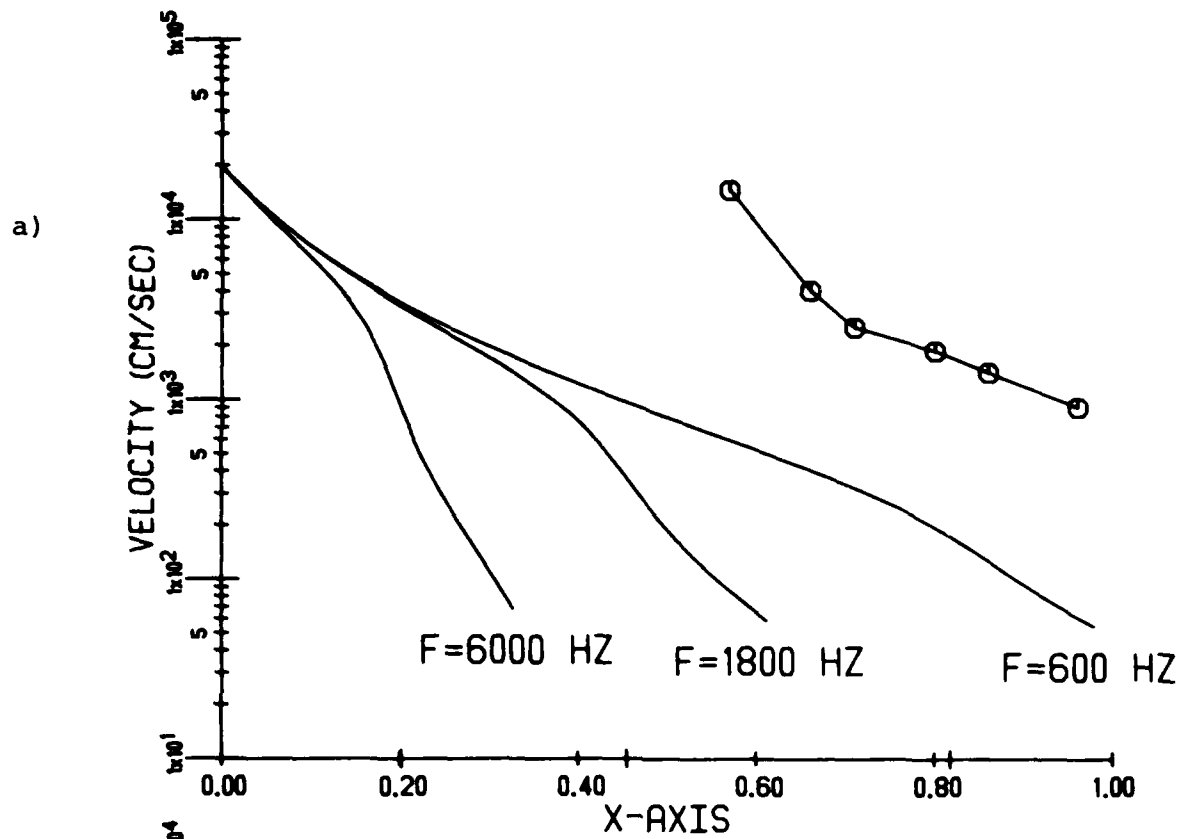FREQUENCY (HZ)

FIG. 7.   The phase velocity of the waves in Figs. 5 and 6.   In
         (a), which corresponds to Fig. 5, the values of von
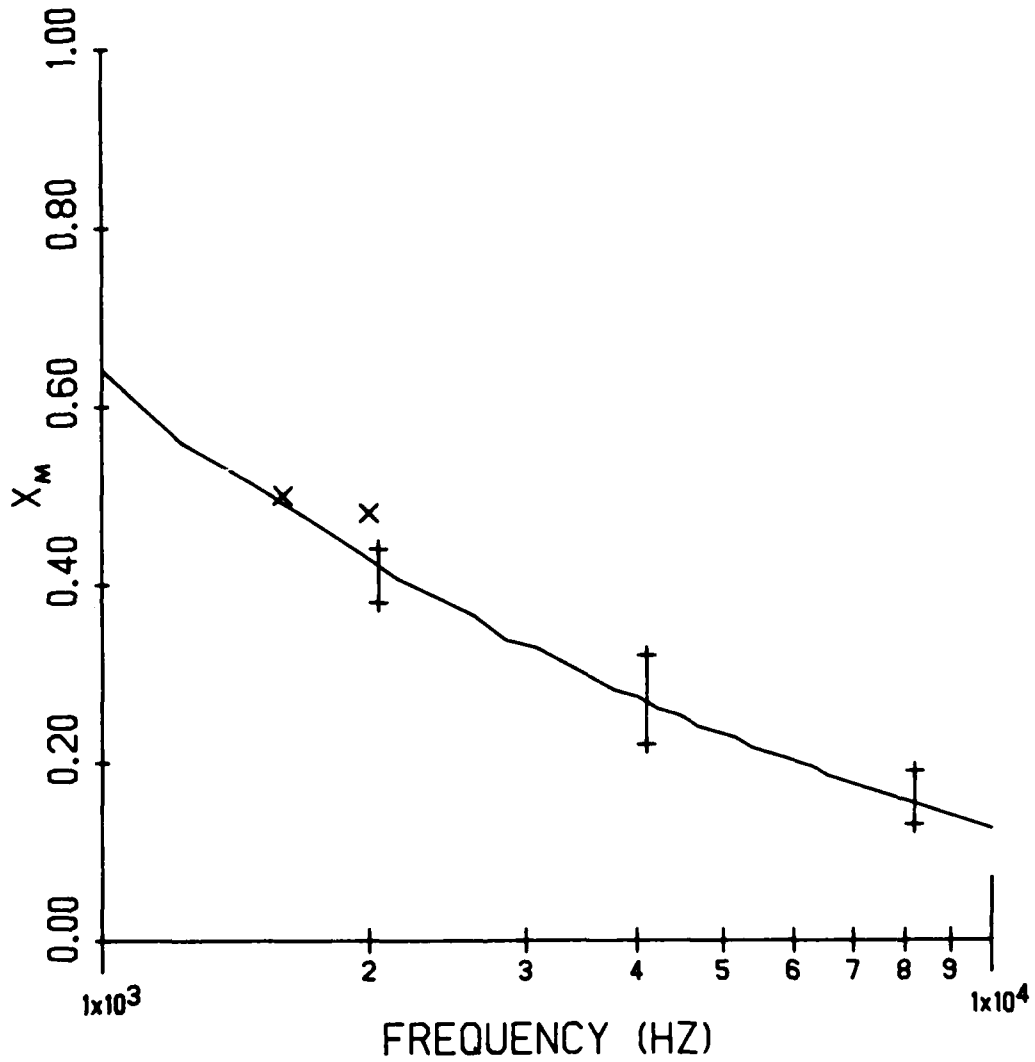   Bekesy are also indicated, with the O.

FIG. 8. The longitudinal location x_M of the maximum amplitude as a function of frequency as determined from the theory (solid curve). Also shown, by the horizontal bars, are the spatial locations measured by Crowe, et al (1934), and von Bekesy's (1960) measurements are given by the x's.

to be a perceivable difference to an observer. It should be
kept in mind in the discussion that such psychoacoustic
measurements are subject to rather significant individual
differences as well as influenced by such things as resonances
of the ear canal (Henning, 1966). In accordance with the place
principle of hearing, we assume that the perceived change in
frequency is due to the shift of the maximum amplitude of the
wave on the basilar membrane. The question is how far does it
have to shift? The answer is related to the stimulation of the
hair cells. There are approximately 3500 rows of such cells
along the membrane, and we assume that the maximum point has to
shift at least the distance of one row before it is possible to
recognize a difference. The resulting difference limen curve is
shown in Fig. 9 along with the experimental results of Wier, et
al (1977), Nordmark (1968) and Shower and Biddulph (1931).
Also included is the curve one would obtain if the shift
required is three rows. All-in-all the agreement between theory
and experiment is very good. It implies that the system is
responsive to very small shifts in the frequency, and the
spatial difference is approximately constant between 1000 and
10,000 Hz. The theoretical curves in the figure can be written
as

$$\log (DL) = 0.023\sqrt{\Omega} + b_0 \quad , \tag{40}$$

where b_0 = -1.08, -0.778, -0.602, -0.477 for shifts of one,
two, three, four hair cell rows, respectively. Interestingly,
the linear relation (40) has been obtained from empirical
curve fits by Wier, et al and also by Nelson, et al (1983).
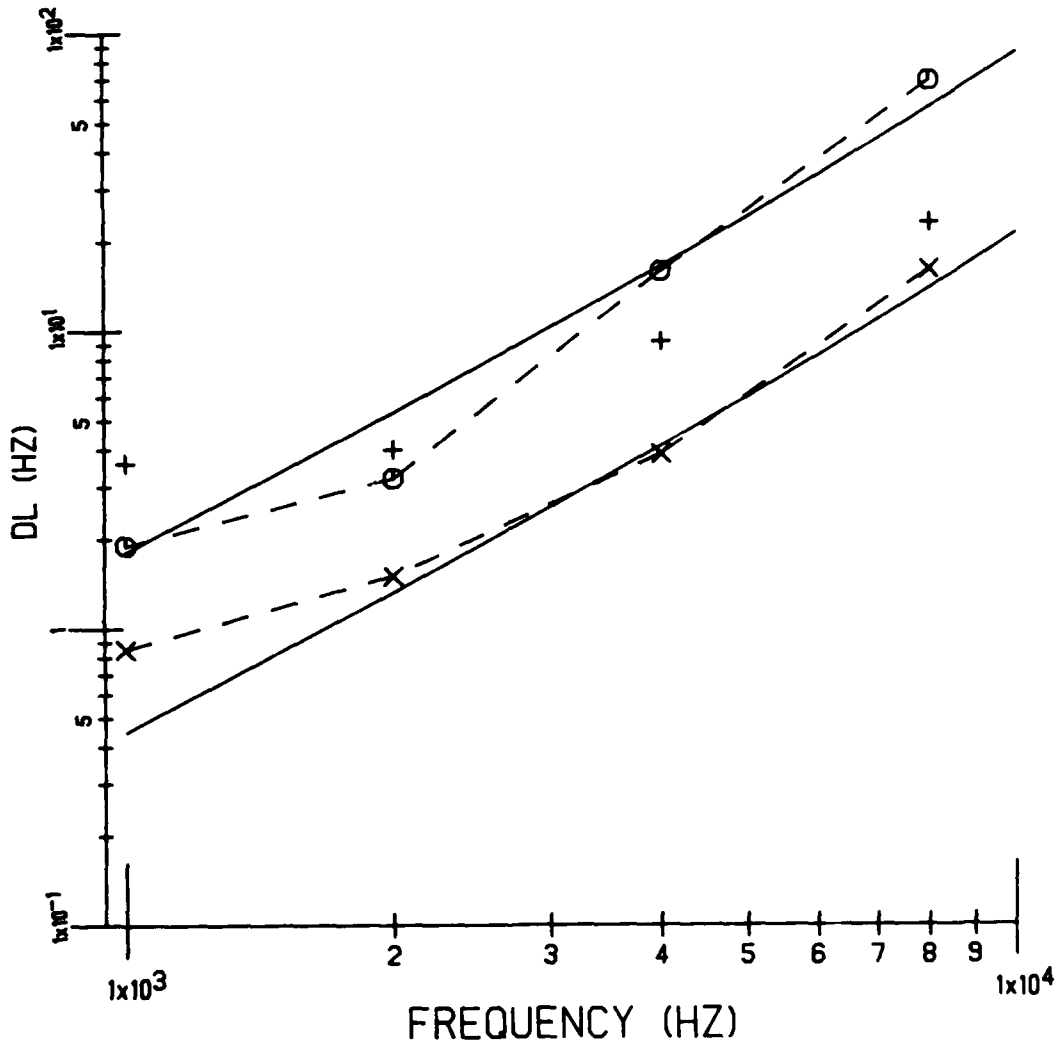
FIG. 9. The difference limen (DL) obtained from the theory for a spatial shift of the maximum amplitude corresponding to a single row of hair cells (lower solid curve) and to three rows of hair cells (upper solid curve). Also shown are the experimental measurements of Shower and Biddulph (1931), with the +, Nordmark (1968), with the x, and Wier, et al (1977), with the O.

The latter show that the slope in (40) is relatively constant as the stimulus sensation level (SL) increases, whereas the intercept b_0 decreases. For SL's between 10 and 80 dB the slope for the data of Nelson, et al, is 0.0214, for Wier, et al, it is 0.0238, and for Harris (1952) it is 0.0235. Clearly, all three slopes are very close to our value of 0.023. As for the decrease of b_0 as the SL increases, this would imply from the theory that a smaller spatial shift is necessary to discern a difference in frequency for a higher SL. This is consistent with the fact that the amplitude on the basilar membrane also increases with the SL, which, in turn, means an increase in the neural signal from the hair cell.

SUMMARY

Using slender body and boundary layer theory we have reduced the three-dimensional hydroelastic model for the cochlea to a nonlinear eigenvalue problem in the transverse cross-section. This problem comes from the strong coupling between the basilar membrane and fluid, and does not exclude any of the effects of the plate, such as the inertia. The subsequent response of the basilar membrane to a pure tone of sufficiently high frequency is a right running wave that begins to grow in amplitude. However, the wavelength decreases and so, due to the viscosity of the fluid, the wave eventually reaches a spatial location after which it quickly decays to zero. For lower frequencies the reflected wave is not negligible particularly in the region near the helicotrema, and has to be included in the solution. This wave would be even more important if there was no damping, as the response to a pure tone would be simply a standing wave and one would obtain resonances corresponding to the eigenvalues of the system (Holmes, 1979).

As outlined at the beginning, there are a number of assumptions made to formulate the model. However, from the resulting analysis, it has been shown to describe a good deal of the qualitative behavior known to occur in the cochlea. Nevertheless, there are a number of interesting extensions of the analysis which could be undertaken. For example, the maximum amplitude on the basilar membrane at, say, 1800 Hz is about 160 times larger than the amplitude of the stapes. This

raises the question as to whether it is necessary to consider a
nonlinear hydroelastic theory in the neighborhood of this point
to account for these relatively large amplitudes. Also, there
has been a question as to where the damping in the system is.
We have only considered the dissipation due to the viscosity
of the fluid, but there surely is damping in the basilar
membrane and its associated structures. This is particularly
true for the short waves which are present on the basilar
membrane on the apical side of the maximum amplitude. It is
not clear exactly how this damping manifests itself but most
of the standard viscoelastic theories can be included in our
analysis without increasingly the difficulty significantly.

APPENDIX A

Derivation of Boundary Condition for the Pressure

The perilymphatic fluid in the upper chamber is assumed to be Newtonian. The equations of motion come from the linearized Navier-Stokes equations and the incompressibility condition which, in scaled coordinates, are

$$(i-\delta^2\nabla^2)\vec{v} = -\nabla p \quad , \tag{A1a}$$

$$\nabla \cdot \vec{v} = 0 \quad . \tag{A1b}$$

To facilitate the presentation we have let $\epsilon = 1$ in (1). Also, the time periodic solution is being considered here.

It follows immediately from (A1) that p satisfies (1a). As for the boundary condition, it is assumed that there is a prescribed normal velocity component as in (2). To give it explicitly let $\vec{x}_0$ be a point on the boundary surface S, which is assumed to be regular in a neighborhood of $\vec{x}_0$. It is then possible to introduce local cartesian coordinates at $\vec{x}_0$ of the form

$$\vec{x} - \vec{x}_0 = s_1\vec{e}_1 + s_2\vec{e}_2 + n\vec{e}_n \quad ,$$

where $\vec{e}_n$ represents the unit outward normal to S at $\vec{x}_0$, and $\vec{e}_1$, $\vec{e}_2$ are in the tangent plane to S at $\vec{x}_0$. Note $\vec{e}_n$, $\vec{e}_1$, $\vec{e}_2$ are independent of the three spatial coordinates. The velocity $\vec{v}$ can now be written as

$$\vec{v} = \vec{v}_s + v_n\vec{e}_n \quad ,$$

where v_n and v_s are the normal and tangential components of v, respectively. The gradient operator can be similarly factored as

$$\nabla = \nabla_s + \vec{e}_n \frac{\partial}{\partial n} \quad .$$

With this, the boundary condition at $\vec{x}_0$ is

$$\vec{v}(\vec{x}_0) = -i n \vec{e}_n \quad . \tag{A2}$$

The fluid motion in the inviscid region is found from (A1) by letting $\delta \to 0$ with $\vec{x}$ fixed in the fluid. The appropriate expansions in this case are

$$\vec{v} \sim \vec{v}_0(s_1, s_2, n) + \delta \vec{v}_1 + \ldots \quad ,$$

and

$$p \sim p_0(s_1, s_2, n) + \delta p_1 + \ldots \quad .$$

From these and (A1) one obtains the following inviscid problems

$$O(1): \quad i\vec{v}_0 = -\nabla p_0 \qquad\qquad O(\delta): \quad i\vec{v}_1 = -\nabla p_1$$

$$\nabla \cdot \vec{v}_0 = 0 \qquad\qquad\qquad\qquad \nabla \cdot \vec{v}_1 = 0 \quad .$$

As is usual, it is impossible to satisfy (A2) with this inviscid approximation, and so, it is necessary to consider the viscous boundary layer on S. With the boundary layer coordinate $\tilde{n} = n/\delta$, the expansions for this region are

$$\vec{v} \sim \vec{V}_0(s_1, s_2, \tilde{n}) + \delta \vec{V}_1 + \ldots \quad , \tag{A3}$$

and

$$P \sim P_0(s_1, s_2, \tilde{n}) + \delta P_1 + \ldots \quad . \tag{A4}$$

Introducing these into (A1) one finds that the first terms in these expansions satisfy

$$\frac{\partial}{\partial \tilde{n}} P_0 = 0 \quad , \qquad \frac{\partial}{\partial \tilde{n}} V_{n0} = 0 \quad ,$$

$$\left(i - \frac{\partial^2}{\partial \tilde{n}^2} \right) \vec{V}_{s0} = -\nabla_s P_0 \quad .$$

Solving these and matching the solutions with the first terms for the inviscid region

$$P_0 = p_0(s_1, s_2, 0) \quad ,$$

$$V_{n0} = -in(s_1, s_2) \quad ,$$

and

$$\vec{V}_{s0} = \vec{v}_{s0}(s_1, s_2, 0)(1 - e^{\sqrt{I} \, \tilde{n}}) \quad .$$

In matching these solutions it is assumed that the fluid lies in the region $n < 0$.

Now, from (A1), (A3), (A4)

$$\frac{\partial}{\partial \tilde{n}} P_1 = -iV_{n0}$$

and

$$\frac{\partial}{\partial \tilde{n}} V_{n1} = -\nabla_s \cdot \vec{V}_{s0} \quad .$$

So, solving and matching with the outer solution

$$P_1 = n\partial_n p_0(s_1,s_2,0) + \tilde{p}_1(s_1,s_2,0)$$

and

$$V_{n1} = -\nabla_s \cdot \vec{v}_{s0}(s_1,s_2,0)[\tilde{n}+(1-e^{-\sqrt{i}\ \tilde{n}})/\sqrt{i}]$$

$$= \partial_n v_{n0}(s_1,s_2,0)[\tilde{n}+(1-e^{-\sqrt{i}\ \tilde{n}})/\sqrt{i}].$$

From this, for the inviscid expansion to match with the one for the boundary layer, v_n must be such that

$$v_n(s_1,s_2,0) \sim -i\eta + \beta\partial_n v_{n0}(s_1,s_2,0) + \ldots \quad .$$

Putting our results together then

$$P(s_1,s_2,\tilde{n}) \sim p_0(s_1,s_2,0)$$

$$+ \delta[\ \tilde{n}\partial_n p_0(s_1,s_2,0) + \tilde{p}_1(s_1,s_2,0)] + \ldots \quad (A5)$$

and

$$\partial_n P(s_1,s_2,0) = -iv_n(s_1,s_2,0)$$

$$= -\eta + \beta\partial_n^2 p_0(s_1,s_2,0) + O(\delta^2)$$

$$= -\eta + \beta\partial_n^2 p(s_1,s_2,0) + O(\delta^2).$$

Therefore,

$$(\partial_n - \beta\partial_n^2)p = -\eta \quad \text{on } S.$$

Also, from (A5) we obtain the pressure on the basilar membrane used in (16).

As is clear from the derivation, these expressions are valid up to $O(\delta^2)$. Moreover, we have used a tangent plane approximation of the surface near $\vec{x}_0$. Given the local nature of the boundary layer this is sufficient but, if a global analysis is desired, one can use orthogonal curvilinear coordinates as presented by Howarth (1959).

APPENDIX B

Solvability Condition

To derive the solvability condition (7), which gives the slow modulation of the wave, we assume here that D_1, D_2, D_k are constants. In this case the $O(\epsilon)$ problem obtained from substituting (3) into (1) is

$$(\partial_y^2 + \partial_z^2 - \Theta_x^2)\overline{p}_1 = -i(\Theta_{xx}\overline{p}_0 + 2\Theta_x \partial_x \overline{p}_0) \quad , \tag{B1}$$

$$P(\zeta_1) - iD_1(4\Theta_x^3 \partial_x \zeta_0 + 6\Theta_x^2 \Theta_{xx} \zeta_0) + 2iD_3 \partial_y^2(2\Theta_x \partial_x \zeta_0 + \Theta_{xx} \zeta_0)$$

$$= -2\omega^2 \overline{p}_1(x,y,0) \quad , \tag{B2}$$

where $P(\cdot)$ represents the differential operator applied to ζ_0 in the $O(1)$ problem (4b). The boundary condition from (2) is

$$(\partial_{n_T} - \beta \partial_{n_T}^2)\overline{p}_1 + i\Theta_x[b\overline{p}_0 - \beta(2b + \overline{p}_0)\partial_{n_T}\overline{p}_0] = \begin{cases} -\alpha \zeta_1 \\ 0 \end{cases} \tag{B3}$$

and the simply supported boundary conditions for the plate give, for $y = G_\pm(x)$,

$$\zeta_1 = \partial_y^2 \zeta_1 - 2i\Theta_x G_x D_3 \partial_y \zeta_0 = 0 \quad . \tag{B4}$$

Now multiplying (B1) by $\overline{p}_0$ and integrating over the cross-section

$$\iint_\Psi \overline{p}_0(\nabla^2 - \Theta_x^2)\overline{p}_1 dy\,dz = -i \iint_\Psi \partial_x(\Theta_x \overline{p}_0^2) dy\,dz$$

$$= -i\frac{d}{dx} \iint_\Psi \Theta_x \overline{p}_0^2 dy\,dz - i\Theta_x \int_{\partial\Psi} b\overline{p}_0^2 \quad .$$

However, using Green's theorem

$$\iint_\Psi \overline{p}_0(\nabla^2 - \Theta_x^2)\overline{p}_1 dy dz = \int_{\partial\Psi}(\overline{p}_0 \partial_{n_T}\overline{p}_1 - \overline{p}_1 \partial_{n_T}\overline{p}_0)$$

$$= -i\Theta_x \int_{\partial\Psi}[b\overline{p}_0^2 - \beta\partial_{n_T}(b\overline{p}_0^2)] + \alpha\int_{G_-}^{G_+}(\zeta_1\overline{p}_0 - \zeta_0\overline{p}_1)dy \quad,$$

where we have also used (B3) and (5). Combining this with the previous result

$$\frac{d}{dx}\iint_\Psi \Theta_x\overline{p}_0^2 dy dz + \beta\Theta_x \int_{\partial\Psi}\partial_{n_T}(b\overline{p}_0^2)$$

$$= \frac{-i\alpha}{2\omega^2}\int_{G_-}^{G_+}[\zeta_1(\zeta_0) - \zeta_0(\zeta_1) + 2iD_1\partial_x(\Theta_x^3\zeta_0^2)$$

$$- 2iD_3\zeta_0\partial_y^2(2\Theta_x\partial_x\zeta_0 + \Theta_{xx}\zeta_0)]dy$$

$$= -\frac{\alpha}{\omega^2}\frac{d}{dx}\int_{G_-}^{G_+}[D_1\Theta_x^3\zeta_0^2 + D_3\Theta_x(\partial_y\zeta_0)^2]dy \quad.$$

where (B4) has been used to obtain the last equality. From this one immediately obtains (7).

APPENDIX C

Solution for a Rectangular Cross-Section

The displacement of a simply supported, homogenous, orthotropic, and centered basilar membrane, as determined by the right running wave, is

$$\eta^*(x,y,t) \sim A_S{}^* A(x) e^{i\left[t-k(x,\varepsilon)-\pi/2\right]} \cos\left(\frac{\pi y}{2G}\right) , \qquad (C1)$$

where

$$k(x,\varepsilon) = \frac{1}{\varepsilon} \int_0^x \left[k_0(s)+\beta_0 k_1(s)\right] ds \qquad (C2)$$

$$A(x) = \frac{A_0}{\sqrt{k_0(x)\iint_\Psi P_0{}^2\, dydz}} \cdot e^{-\frac{1}{\varepsilon}\beta_0\int_0^x k_1(s)ds} , \quad (C3)$$

$$A_0 = \frac{\pi A_w k_0(0)}{4G(0)} \sqrt{k_0(0)\iint_\Psi P_0(0,y,z)^2\, dydz} . \qquad (C4)$$

The parameters are (Figs. 1,2)

$$\varepsilon = \frac{B}{L} , \quad \beta_0 = \sqrt{\frac{\nu}{4\pi f B^2}} , \quad \alpha = \frac{\rho B}{\mu}$$

and

$$\omega = 2\pi f \sqrt{\frac{\mu B^4}{D}} .$$

Here f is the driving frequency (in Hz), $A_S{}^*$ is the amplitude of the stapes, and $A_w = (A_w{}^*/B^2)$ is the dimensionless area of the oval window.

For the case of a rectangular cross-section, the eigenvalue $k_0(x)$ is found by solving the equation

$$D_1 k_0^4 + 2D_3 \omega_r k_0^2 + \omega_r^2 - \omega^2 = \frac{1}{G} \sum_{m=0}^{\infty} a_m K_{m1}^2 \quad,$$

where

$$\omega_r = \left(\frac{\pi}{2G}\right)^2 \quad,$$

$$a_m = \frac{2\alpha\omega^2 c_m}{\lambda_m \tanh \lambda_m H} \quad,$$

$$\lambda_m = \sqrt{k_0^2 + \gamma_m^2} \quad, \quad \gamma_m = \frac{m\pi}{H} \quad,$$

$$c_m = \begin{cases} \dfrac{1}{2H} & \text{if } m=0 \\[2ex] \dfrac{1}{H} & \text{if } m \neq 0 \end{cases}$$

and

$$K_{m1} = \begin{cases} \dfrac{2\sqrt{\omega_r} \cos \gamma_m G}{\omega_r - \gamma_m^2} & \text{if } \gamma_m^2 \neq \omega_r \\[2ex] G & \text{if } \gamma_m^2 = \omega_r \end{cases} \quad.$$

In these expressions, D_1 and D_2 are constants but G and H are functions of x (as determined by the geometry).

Once k_0 is found, the function $k_1(x)$ in (C2) and (C3) is found from (16). To do this note, from (17), that

$$p_0(x,y,z) = \sum_{m=0}^{\infty} \bar{p}_m \cosh \lambda_m (H-z) \cos \gamma_m y \quad, \tag{C5}$$

where

$$\bar{p}_m = \frac{-\alpha c_m K_{m1}}{\lambda_m \sinh \lambda_m H} \quad .$$

Thus,

$$k_1(x) = k_0(x) \left[\frac{H \sum\limits_{m=0}^{\infty} \bar{p}_m^2 (1+\cosh^2 \lambda_m H) + \sum\limits_{m=0}^{\infty} \sum\limits_{n=0}^{\infty} (-1)^{n+m} \bar{p}_m \bar{p}_n L_{mn}}{H \sum\limits_{m=0}^{\infty} \bar{p}_m^2 \left(H + \frac{1}{2\lambda_m} \sinh 2H\lambda_m \right) + \frac{2\alpha}{\omega^2} (D_1 k_0^2 + D_3 \omega_r)G} \right]$$

where

$$L_{mn} = \begin{cases} \dfrac{\sinh(\lambda_n+\lambda_m)H}{\lambda_n+\lambda_m} + \dfrac{\sinh(\lambda_n-\lambda_m)H}{\lambda_n-\lambda_m} & \text{if } n \neq m \\[2em] H + \dfrac{1}{2\lambda_n} \sinh 2\lambda_n H & \text{if } n=m \quad . \end{cases}$$

The denominator of the coefficient of the exponential in (C3) can be calculated from the relation

$$\iint\limits_{\Psi} p_0^2 \, dydz = \frac{1}{2} H \sum_{m=0}^{\infty} \bar{p}_m^2 \left(1 + \frac{1}{2\lambda_m} \sinh 2\lambda_m H\right) \quad .$$

This, at the same time, determines the constant A_0 in (C4).

The displacement of the basilar membrane is completely determined from the above formulas. As for the fluid pressure

$$p^*(x,y,z,t) \sim A_s^* (4\pi^2 \mu f^2) A(x) e^{i[t-k(x,\epsilon)-\pi/2]} p_0(x,y,z)$$

where $p_0(x,y,z)$ is given in (C5). From this one can calculate the velocity $\vec{v}^*(x,y,z,t)$ of the fluid, away from the immediate

vicinity of the cochlear wall with the relation

$$\vec{v}^* = \frac{i}{2\pi f} \nabla^* p^* \quad .$$

REFERENCES

Adjemian, B.C. (1981). A Three Chamber Model of the Cochlea. Ph.D. Thesis, University of California, Los Angeles.

Bekesy, G. (1960). Experiments in Hearing. Krieger Pub., New York.

Chadwick, R.S. (1980). "Studies in cochlear mechanics," Mathematical Modeling of the Hearing Process. (M. Holmes and L. Rubenfeld eds.). Springer-Verlag Lecture Notes in Biomath., New York, 9-54.

Chadwick, R.S. and Cole, J.D. (1979). "Modes and waves in the cochlea," Mech. Res. Comm 6, 177-184.

Crowe, S., Guild, S. and Polvogt, L. (1934). "Observations on the pathology of high-tone deafness," Bull. Johns Hopkins Hosp. 54, 315-379

Frommer, G.H. (1979). "Fluid motion in the mammalian organ of Corti: a possible source of the second filter," Acta Oto-Lary. Supp. 363.

Geisler, C.D., Rhode, W.S., and Kennedy, D.K. (1974). "The responses to tonal stimuli of single auditory nerve fibers and their relations to basilar membrane motion in the squirrel monkey," J. Neurophysiol. 37, 1156-1172.

Harris, J.D. (1952). "Pitch discrimination," J. Acoust. Soc. Am. 24, 750-755.

Henning, G.B. (1966). "Frequency discrimination of random-amplitude tones," J. Acoust. Soc. Am. 39, 336-339.

Holmes, M.H. (1979). "A spectral problem in hydroelasticity," J. Diff. Eqs. 32, 388-397.

Holmes, M.H. (1980). "An analysis of a low frequency model of the cochlea," J. Acoust. Soc. Am. 67, 482-488.

Holmes, M.H. (1982). "A mathematical model of the dynamics of the inner ear," J. Fluid Mech. 116, 59-75.

Howarth, L. (1959). "Laminar boundary layers," Handbook of
    Physics (S. Flugge ed.). Springer-Verlag, Berlin 264-350.

Iurato, S. (1967). Submicroscopic structure of the inner ear.
    Pergamon Press, London.

Johnstone, B.M. and Boyle, A.J.F. (1967). "Basilar membrane
    vibrations examined with the Mossbauer technique," Science
    158, 390-391.

Kiang, N.Y.S., Watanabe, T., Thomas, E.C. and Clark, L.F.
    (1965). "Discharge patterns of single fibers in the cat's
    auditory nerve," M.I.T. Research Monogr. 35, Cambridge, Mass.

Khanna, S.M. (1983). "Interpretation of the sharply tuned
    basilar membrane response observed in the cochlea," Hearing
    and Other Senses (R.R. Fay and G. Gourevitch, eds.) The
    Amphora Press, Groton, 65-86.

Khanna, S.M. and Leonard, D.G.D. (1981). "Basilar membrane
    response measured in damaged cochleas of cats," Mathematical
    Modeling of the Hearing Process (M. Holmes and L. Rubenfeld
    eds). Springer-Verlag Lecture Notes in Biomath, New York,
    70-84.

Khanna, S.M. and Leonard, D.G.D. (1982). "Basilar membrane
    tuning in the cat cochlea," Science 215, 305-306.

Khanna, S.M. and Leonard, D.G.D. (1983). "Cochlear damage
    incurred during preparation for and measurement of basilar
    vibrations," to appear.

Kliauga, P. and Khanna, S.M. (1983). "Dose rate to the inner
    ear during Mossbauer experiments," Phys. Med. Biol. 28,
    359-366.

Lekhnitskii, S.G. (1968). Anisotropic Plates. Gordon and
    Breach, New York.

Lighthill, J. (1981). "Energy flow in the cochlea," J. Fluid
    Mech. 106, 149-213.

Lighthill, J. (1983). "Advantages from describing cochlear
    mechanics in terms of energy flow," Mechanics of Hearing
    (E. de Boer and M.A. Viergever, eds). Martinus Nijhoff,
    Delft University Press, Delft, 63-71.

Money, K.E., Sokoloff, M. and Weaver, R.S. (1966). "Specific gravity and viscosity of endolymph and perilymph," Second Sym. on Role of Vestibular Organs in Space Exploration, NASA SP-115, 91-98.

Nelson, D.A., Stanton, M.E. and Freyman, R.L. (1983). "A general equation describing frequency discrimination as a function of frequency and sensation level," J. of Acoust. Soc. Am. 73, 2117-2123.

Nordmark, J.O. (1968). "Mechanisms of frequency discrimination" J. Acoust. Soc. Am. 44, 1533-1537.

Novoselova, S.M. (1975). "The basilar membrane as an elastic plate," Sov. Phys. Acoust. 21, 56-60.

Rauch, S. and Rauch, I. (1974). "Physico-Chemical Properties of the Inner Ear, Especially Ionic Transport," Handbook of Sensory Physiology (W. Keidel and W. Neff eds). Springer-Verlag, New York, 647-682.

Rhode, W.S. (1971). "Observations of the vibration of the basilar membrane in squirrel monkey using the Mossbauer technique," J. Acoust. Soc. Am. 49, 1218-1231.

Russell, I.J. and Sellick, P.M. (1978). "Intracellular studies of hair cells in the mammalian cochlea," J. Physiol. 284, 261-290.

Schuknecht, H.F. (1970). "Pathophysiology of the fluid systems of the inner ear," Contributions to Sensory Physiology (W. Neff ed.). Academic Press, New York, 75-93.

Shower, E.G. and Biddulph, R. (1931). "Differential pitch sensitivity of the ear," J. Acoust. Soc. Am. 3, 275-287

Steele, C.R. (1974). "Behavior of the basilar membrane with pure tone excitation," J. Acoust. Soc. Am. 55, 148-162.

Steele, C.R. (1976). "Cochlear Mechanics," Handbook of Sensory Physiology (W. Keidel and W. Neff eds.). Springer-Verlag, New York, 443-478.

Steele, C.R. (1980). "Lecture Notes on Cochlear Mechanics," NSF-CBMS Conf. on Math Modeling of the Hearing Process, Troy, New York.

Steele, C.R. and Taber, L.A. (1979). "Comparison of WKB calculations and experimental results for three-dimensional cochlear models," J. Acoust. Soc. Am. 65, 1007-1018.

Voldrich, L. (1978). "Mechanical properties of basilar membrane," Acta Otolaryngol. 86, 331-335.

Wier, C.C., Jesteadt, W. and Green, D.M. (1977). "Frequency discrimination as a function of frequency and sensation level," J. Acoust. Soc. Am. 61, 178-184.

Zwislocki, J. (1965). "Analysis of some auditory characteristics," Handbook of Math. Psychology (R. Luce, R. Bush, and E. Galanter eds.). Wiley, New York, 1-97.

Zwislocki, J. (1980). "Two possible mechanisms for the second cochlear filter," Psychophysical, Physiological, and Behavioural Studies in Hearing (G. van den Brink and F. Bilsen eds.). Delft Univ. Press, 16-23.

REPORT DOCUMENTATION PAGE		READ INSTRUCTIONS BEFORE COMPLETING FORM
1. REPORT NUMBER R.P.I. Math Report No. 139	2. GOVT ACCESSION NO. AD-A136438	3. RECIPIENT'S CATALOG NUMBER
4. TITLE (and Subtitle) Cochlear Mechanics: Analysis for a Pure Tone		5. TYPE OF REPORT & PERIOD COVERED 6. PERFORMING ORG. REPORT NUMBER
7. AUTHOR(s) Mark H. Holmes and Julian D. Cole		8. CONTRACT OR GRANT NUMBER(s) DAAG29-83-K-0092
9. PERFORMING ORGANIZATION NAME AND ADDRESS Rensselaer Polytechnic Institute Troy, N.Y. 12181		10. PROGRAM ELEMENT, PROJECT, TASK AREA & WORK UNIT NUMBERS
11. CONTROLLING OFFICE NAME AND ADDRESS U. S. Army Research Office Post Office Box 12211 Research Triangle Park, NC 27709		12. REPORT DATE Nov. 7, 1983
		13. NUMBER OF PAGES 55
14. MONITORING AGENCY NAME & ADDRESS(if different from Controlling Office)		15. SECURITY CLASS. (of this report) Unclassified
		15a. DECLASSIFICATION/DOWNGRADING SCHEDULE

16. DISTRIBUTION STATEMENT (of this Report)

Approved for public release; distribution unlimited.

17. DISTRIBUTION STATEMENT (of the abstract entered in Block 20, if different from Report)

NA

18. SUPPLEMENTARY NOTES

The view, opinions, and/or findings contained in this report are those of the author(s) and should not be construed as an official Department of the Army position, policy, or decision, unless so designated by other documentation.

19. KEY WORDS (Continue on reverse side if necessary and identify by block number)

20. ABSTRACT (Continue on reverse side if necessary and identify by block number)

The dynamical response of a three-dimensional hydroelastic model of the cochlea is studied for a pure tone forcing. The basilar membrane is modeled as an inhomogenous, orthotropic

elastic plate and the fluid is assumed to be Newtonian. The resulting mathematical problem is reduced using viscous boundary layer theory and slender body approximations. This leads to a nonlinear eigenvalue problem in the transverse cross-section. The solutions for the case of a rectangular and semi-circular cross-section are computed and comparison is made with experiment. The role of the place principle in determining the difference limen is presented and it is shown how the theory agrees with the experimental measurements.

LMED

8